

# Grover's Search-Inspired Quantum Reinforcement Learning for Massive MIMO User Scheduling

Ruining Fan <sup>\*</sup>, Xingyu Huang <sup>†</sup>, Mouli Chakraborty <sup>‡</sup>, Avishek Nag <sup>§</sup>, Anshu Mukherjee <sup>\*</sup>

<sup>\*</sup> School of Electrical and Electronic Engineering, University College Dublin, Belfield, Dublin 4, Ireland

<sup>†</sup>Department of Electrical and Electronic Engineering, Imperial College London, South Kensington, London, UK

<sup>‡</sup> School of Computer Science and Statistics, Trinity College Dublin, The University of Dublin, College Green, Dublin 2, Ireland

<sup>§</sup> School of Computer Science, University College Dublin, Belfield, Dublin 4, Ireland

Email: ruining.fan@ucdconnect.ie, anshu.mukherjee@ieee.org

**Abstract**—The efficient user scheduling policy in the massive Multiple Input Multiple Output (mMIMO) system remains a significant challenge in the field of 5G and Beyond 5G (B5G) due to its high computational complexity, scalability, and Channel State Information (CSI) overhead. This paper proposes a novel Grover's search-inspired Quantum Reinforcement Learning (QRL) framework for mMIMO user scheduling. The QRL agent can explore the exponentially large scheduling space effectively by applying Grover's search to the reinforcement learning process. The model is implemented using our designed quantum-gate-based circuit, which imitates the layered architecture of reinforcement learning, where quantum operations act as policy updates and decision-making units. Moreover, the simulation results demonstrate that the proposed method achieves proper convergence and significantly outperforms classical Convolutional Neural Networks (CNN) and Quantum Deep Learning (QDL) benchmarks by 51% and 43%, respectively.

**Index Terms**—Massive MIMO, User Scheduling, Quantum Reinforcement Learning, Grover's Search, 5G/B5G Networks, Quantum Communication

## I. INTRODUCTION

Efficient user scheduling remains one of the most highly anticipated algorithmic challenges in mMIMO systems. Conventional approaches, while effective in small-scale deployments, suffer from high complexity, limited scalability, and significant CSI overhead in large antenna-user configurations [1].

Existing works address the problem using various methods, including traditional Machine Learning (ML)-based solutions and some quantum computation-assisted proposals. Due to the constrained computational capabilities of the Base Station (BS)s, traditional approaches are restricted to forecasting the CSI for upcoming time intervals solely based on the existing dataset. To maintain accuracy, previous studies often require supplementary methods, such as long short-term memory networks [2], for support. Powered by the quantum-based algorithm, the CSI database traversal becomes more achievable, resulting in a higher average sum rate for hybrid quantum communication systems compared to works that use traditional ML methods. Some representative papers and their adopted methods are listed in Table 1 for visual comparison. The unique method adopted by our paper is also illustrated, showcasing our originality.

Among various quantum algorithms, Grover's search is particularly suitable for the massive MIMO user scheduling

TABLE I: Representative Works Methods Comparison

Papers	[3]	[4]	[5]	Our Work
Deep Learning	✓		✓	
Reinforcement Learning		✓		✓
Quantum Computing Powered			✓	✓

problem, since it can quadratically speed up exploration of unstructured solution spaces. The scheduling task can be viewed as a combinatorial search for optimal user-antenna allocations, where Grover's amplitude amplification could highlight the high-reward policies effectively. Additionally, the oracle can also ensure the exploration-exploitation trade-off in reinforcement learning, making it a natural foundation for our proposed QRL scheme.

In this paper, we propose a novel solution by adopting QRL for mMIMO user scheduling. QRL leverages the interplay between reinforcement learning and quantum-inspired search mechanisms to navigate and traverse the exponentially large scheduling space more efficiently. Grover's Search Algorithm is one of the most essential QRL-based searching algorithms, which establishes a quantum search technique that can amplify the probability of finding optimal solutions within an unsorted database quadratically faster than classical algorithms [6]. Incorporating this principle within the reinforcement learning framework, the QRL agent investigates potential scheduling strategies in a manner enhanced by quantum computing. Here, the oracle identifies feasible solutions, and amplitude amplification directs the learning path towards nearly optimal policies. In terms of implementation, we designed a quantum gate-based circuit which imitates the function of the layered structure of a reinforcement learning architecture, where one-to-one quantum operations play the role of decision maker and policy updates. This integration enables our system to reduce the computational burden of CSI traversal and to converge faster toward high-throughput scheduling strategies, thereby overcoming the scalability barrier faced by classical methods. Additionally, it also laid the foundation for Grover's search-inspired quantum communication algorithm, which could play a significant role in the fields of 5G and B5G. To sum up, the novelty and contribution of this paper can be summarized as follows:

- Grover-inspired QRL framework for user scheduling: We propose a novel quantum-circuit-based QRL method for mMIMO user scheduling, where the circuit is integrated with conventional reinforcement learning principles. The design enhances the traversal speed of the computational task, thereby increasing the system's scalability. Simultaneously, the system achieves near-optimal scheduling with higher throughput than classical methods.
- Perform evaluation and scalability illustration: The proposed QRL model is compared with conventional CNN and Quantum Neural Networks (QNN) [5] benchmarks under various scenarios. The scalability of our method is demonstrated by consistently achieving higher average sum rates as the user-antenna configurations are scaled up. The robustness of the system is potentially essential for B5G networks.

In the remaining sections, we present the detailed design of the proposed algorithm, followed by numerical analysis and comparative evaluation against existing methods.

## II. SYSTEM MODEL

In this paper, a single-cell massive MIMO downlink system is considered. The system contains  $A$  antennas at the BS, which serves  $T$  terminal users with a single antenna. For each user, the downlink channel is denoted as  $\mathbf{n}_t \in \mathbb{C}^A$ . Although the antenna configurations at the BS have flexibility, we adopt the rectangular configuration in this work: The BS contains  $X$  rows of antenna strings and  $Y$  antennas are there in each row. Note that the number of users who are served by the BS simultaneously  $T \leq A = X \cdot Y$ .

### A. Received Signals and Ergodic Sum Rate

In the focused multiuser downlink system, the received signal at each terminal user  $t$  can be presented as

$$\mathbf{y}_t = \mathbf{n}_t \cdot \mathbf{x} + \mathbf{g}_t, \quad (1)$$

where  $\mathbf{x} = \sum_{t=1}^T \sqrt{p_t} \cdot \mathbf{s}_t$  are the signals transmitted through all the antennas in the BS, with  $\mathbb{E}[|\mathbf{s}_t|^2] = 1$  being the data symbols of user  $t$ . The noise component  $\mathbf{g}_t$  follows the pattern of Additive White Gaussian Noise (AWGN) that  $\mathbf{g}_t \sim \mathcal{CN}(0, \sigma_t^2)$ . For the sake of fairness for every user in the system, we assume each user gets the same amount of energy  $P = \sqrt{p_t} = \sqrt{P_{total}/T}, \forall t$  [7].

Furthermore, the ergodic sum rate can be presented as

$$S_{sum} = \sum_{t=1}^T S_t, \quad (2)$$

where  $S_t$  is the so-called ergodic rate, which is deduced by the Shannon capacity and the corresponding concept of Signal-to-interference-plus-noise Ratio (SINR) [8]:

$$S_t \approx \log_2[1 + \mathbb{E}_t(\text{SINR}_t)]. \quad (3)$$

Since we are dealing with the large-scale Grover's search problem in this paper, which will be discussed in the upcoming section, we can use the approximation form of the ergodic rate for each given user  $t$  without affecting the final training outcome of our proposed system.

### B. Beam Domain Channel State Information

Compared to the Rayleigh fading channel conditions that are used widely in large-scale MIMO systems, the Rician fading channel model has a Rician-K factor which balances the channel conditions between pure Line of Sight (LoS) and full scattering [7]. It gives more robustness to our proposed algorithm by yielding a flexible feedback under structured channels. Originally, the stacked channel of the system is written as

$$\mathbf{N} = [\mathbf{n}_1, \dots, \mathbf{n}_u] \in \mathbb{C}^{A \times T}, \quad (4)$$

which is known as conventional CSI. In the considered correlated Rician fading channel, we define the channel vector as

$$\mathbf{N}_t^r = \tilde{\mathbf{K}} \cdot \mathbf{n}_t^{LoS} + \hat{\mathbf{K}} \cdot \mathbf{n}_t^{NLoS} \sqrt{\mathbf{M}_t}, \quad (5)$$

where  $\tilde{\mathbf{K}}$  and  $\hat{\mathbf{K}}$  are the coefficients which are deducted from the Rician K-factor,  $\mathbf{n}_t^{LoS} \in \mathbb{C}^{T \times 1}$  denotes the LoS channel vector components, with  $\mathbf{n}_t^{NLoS}$  representing the Non Line-of-sight (NLoS) mean-centred components with normalized variance [9]. Moreover,  $\mathbf{M}_t \in \mathbb{C}^{T \times T}$  is the channel correlation matrix of the NLoS components.

Now, with the assistance of the Rician fading channel, equation (1) can be represented in a detailed and beam-forming manner [7]:

$$\begin{aligned} \mathbf{y}_t &= \sum_{t=1}^T P \mathbf{N}_t^r \mathbf{f}_t S_t + \mathbf{g}_t \\ &= P \mathbf{N}_t^r \mathbf{f}_t S_t + \sum_{x=1, x \neq t}^T P \mathbf{N}_x^r \mathbf{f}_x S_x + \mathbf{g}_t, \end{aligned} \quad (6)$$

note that the  $\mathbf{f}_t \in \mathbb{C}^{T \times 1}$  is the beamforming vector. Generally, it can be approximated by utilizing the unitary Discrete Fourier Transform (DFT)  $\Omega_T$  and its conjugate transpose to calculate the diagonal matrix:

$$\mathbf{D}_t = \Omega_T^H \mathbb{E}[\|\mathbf{N}_t^r\|_2^2] \Omega_T, \quad (7)$$

which the  $i_t$ -th largest diagonal element corresponds to the  $j_t$ -th in the DFT matrix, which maximizes the energy in a particular direction for an aimed terminal user [10]. Therefore, the BS will choose the column as the optimal beamforming vector  $\mathbf{F}_t$  for the user accordingly.

### C. Proportional Fairness-inspired Problem Formulation

In this paper, the optimal goal is to schedule users in the targeted mMIMO downlink system so that the entire system can achieve a better sum rate without compromising fairness. Firstly, a scheduling vector is necessary

$$\theta(t) = \{\theta^1(t), \dots, \theta^T(t)\} \in \{0, 1\}^T, \quad (8)$$

each scheduling indicator  $\theta^t(\cdot) = 1, \forall t, t < T$  means the corresponding user is scheduled during the current time slot. From equation (3), the instantaneous achievable rate can be calculated as [5]

$$\hat{S}_t(t) = \log_2 \left( \frac{\sum_{\gamma=1}^T \mathbf{f}_t \theta^\gamma(t) + 1}{\sum_{\gamma=1, \gamma \neq t}^T \mathbf{f}_t \theta^\gamma(t) + 1} \right). \quad (9)$$

To strike a balance between fairness and channel capacity utilization rate, we choose the Proportional Fairness (PF) method to ensure fairness for each user. Thus, the problem can now be written as

$$\{\theta^1(t), \dots, \theta^T(t)\} \underset{\text{argmax}}{\sum_{\gamma=1}^T} \frac{\hat{\mathbf{S}}_\gamma(t)}{\bar{\mathbf{S}}_\gamma(t+1) + a},$$

$$\bar{\mathbf{S}}_\gamma(t+1) = \begin{cases} (1-\omega)\bar{\mathbf{S}}_\gamma(t) + \omega\hat{\mathbf{S}}_\gamma(t), & \text{if } \theta^t(t) = 1, \\ \bar{\mathbf{S}}_\gamma(t), & \text{otherwise.} \end{cases} \quad (10)$$

Note that the time  $(t+1)$  represents the long-term achievable ergodic sum rate, and  $\omega \in (0, 1)$  is the forgetting factor for the historical rate, and  $a$  is just a small number that prevents the division by zero problem.

### III. PROPOSED QUANTUM REINFORCEMENT LEARNING METHOD

#### A. Grover's Search Quantum Circuit

Grover's search is an algorithm that utilizes quantum superposition and parallelism. It can traverse the database quadratically faster than classical computers can in terms of time, assisted by the quantum circuit [11]. In this section, we provide a detailed description of our designed Grover's search quantum circuit. The abstract architecture is illustrated in Fig. 1, with solid lines representing its three main layers.

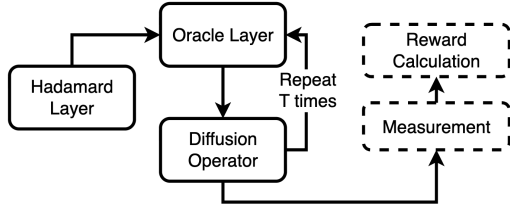


Fig. 1: Grover's search-based quantum circuit architecture.

Firstly, the initial superposition layer, also known as the Hadamard layer, is responsible for initializing the state of each input qubit. Hadamard gates create a uniform superposition over all possible states, so that the Grover's agent can search the entire solution space in parallel [12]. Since we have  $T$  users in the targeted system, we require the same number of Hadamard gates and wires accordingly. In the beginning,  $N = T$  qubits are used to encode all the users,

$$|\psi_0\rangle = |0\rangle^{\otimes N}, \quad (11)$$

which are then fed to the Hadamard gates with the corresponding dimension, and we get

$$|\psi_1\rangle = H^{\otimes N} |\psi_0\rangle = \mathcal{A} \sum_{i=0}^{2^N-1} |\theta\rangle, \quad (12)$$

where  $\mathcal{A} = \frac{1}{\sqrt{2^N}}$ , is the uniformed probability amplitude for each superposed states.  $|\theta\rangle = |\theta^1\theta^2\dots\theta^N\rangle$  is the computational basis states, converted from the scheduling vector in equation (8).

Furthermore, in the second oracle layer, some positive action in the iteration will be marked, which is done by flipping the phase of the states using Pauli-X pre-processing and a followed multi-controlled Z gate. The marked states are stored in a space  $\mathcal{M} \subseteq \{0, 1\}^N$ , and the oracle marking action obeys the rule

$$\mathcal{O}_{\mathcal{M}} |\theta\rangle = \begin{cases} -|\theta\rangle, & \theta \in \mathcal{M}, \\ |\theta\rangle, & \theta \notin \mathcal{M}. \end{cases} \quad (13)$$

Moreover, the diffusion operator layer mirrors and reflects the oracles from the last layer, but centered around the uniform state. This layer mainly relies on a diffusion operator, which is defined as

$$\text{Diff} = 2 \cdot |U\rangle\langle U| - I. \quad (14)$$

Note that  $|U\rangle$  is the uniform state that comes from equation (12), and  $I$  denotes the identity matrix. It ensures the core amplification steps in Grover's search, which perform inversion about the mean [11].

To summarise, the detailed design of the proposed Grover's search quantum circuit is illustrated in Fig. 2, which uses only 5 qubits for simplicity and can be extended to higher dimensions.

#### B. Proposed Quantum Reinforcement Learning Algorithm

In this section, the method for training the aforementioned QRL model is discussed. In Algorithm 1, the essential training steps are listed in detail. The model takes a basic Grover vector  $\mathbf{G}\{\mathcal{S}, \mathcal{K}, \mathcal{R}\}$ , meaning current state, amplify factor, and reward correspondingly, along with other training parameters such as the one that defines the iteration number, batch size, learning rate, and most importantly, the oracle threshold  $\tau$ . In terms of the output, it will return the measured and collapsed scheduling vector  $\theta(t)$  for an instantaneous time interval. Initially, the model parameters, including those of the optimizer, are set to their initial state without any bias. Secondly, within each training batch, the scheduling indicators pass through the Hadamard layer, where the vectors are superposed and mapped into the Hilbert space with uniform probability amplitudes. In the second layer, each strategy is evaluated through the oracle, which computes the instantaneous sum rate as the reward of the current epoch. Then, the third step will examine whether the reward is greater than the predefined threshold  $\tau$ ; if so, the third layer, as mentioned in the last section, will take action to mark the action with a high reward via phase inversion. Ultimately, the amplitude amplification step updates the trainable parameters to increase the probability of measuring optimal policies across iterations. Finally, after the current strategy is measured in the vector space, the validation reward is determined based on this, which is logged for monitoring purposes. The same procedure will continue until the model's performance has converged.

## IV. RESULTS

To evaluate our proposed QRL model and its training outcomes, we first ensure that the model is properly converged, and then it is compared with the traditional CNN benchmark and another QDL scheme, as discussed in [5].

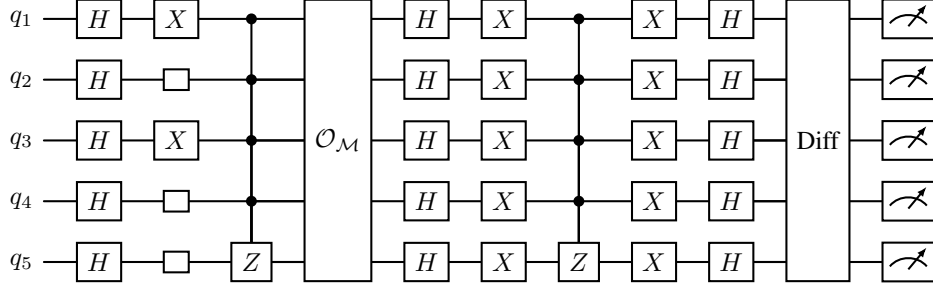


Fig. 2: Grover-based Quantum Circuit (5 qubits).

**Algorithm 1** Grover-inspired QRL Training for User Scheduling

**Require:** Initial QRL parameters  $\mathbf{G}\{\mathcal{S}, \mathcal{K}, \mathcal{R}\}$ , learning rate  $\eta$ , batch size  $B$ , epochs  $N_{\text{epochs}}$ , Grover iterations per batch  $G$ , oracle threshold  $\tau$

**Ensure:** Trained QRL model with near-optimal scheduling policy  $\theta(t)$

- 1: Initialize QRL parameters  $\mathbf{G}$
- 2: Initialise optimiser
- 3: **for** epoch = 1 to  $N_{\text{epochs}}$  **do**
- 4:   **for** each batch of training samples **do**
- 5:     Prepare uniform superposition of candidate policies  $\theta \leftarrow \text{QRL}(\mathbf{A}; \mathbf{G})$
- 6:     **Oracle:** evaluate reward:  
       $\mathcal{R} \leftarrow \text{calculate\_sum\_rate}(\mathbf{A}, \theta(t), \sigma^2)$
- 7:     **if**  $\mathcal{R} \geq \tau$  **then**
- 8:       Mark high-reward policies via phase inversion
- 9:     **end if**
- 10:    **Amplitude amplification:** update  $\mathcal{K}$  to amplify marked policies
- 11:   **end for**
- 12:   Measure  $\theta(t)$  to collapse into best scheduling policy
- 13:   Log validation reward
- 14: **end for**
- 15: **return** trained QRL model

To begin with, the training curve shown in Fig. 3 clearly demonstrates the proper convergence behavior of the designed Grover-inspired QRL model. The curve starts from an initial average sum rate of 22 bps/Hz, the agent shows a steady increase in performance throughout the 500 training epochs, ultimately reaching close to 32 bps/Hz. During the early 200 epochs, the higher slope of the curve highlights the model's capability to rapidly improve its policy, while the gradual flattening of the curve beyond epoch 350 indicates that the learning process stabilises and approaches a plateau. In terms of the oscillation, it can be seen that as the epoch number increases, there are fewer fluctuations, confirming that the agent is approaching a near-optimal scheduling policy and also demonstrating the exploration-exploitation trade-off. Now, we move on to the benchmark comparison section. Firstly, we

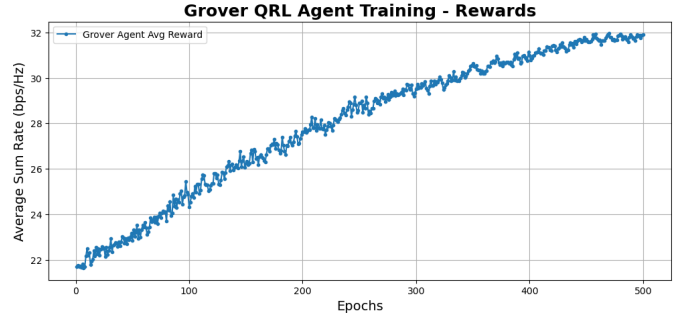


Fig. 3: Training convergence of the Grover-inspired QRL agent showing steady reward growth and stabilization.

consider the scenario that in a mMIMO system, the antenna number at the BS is fixed, and what would be the performance difference between QRL, QNN and traditional CNN benchmark under different user loads. As illustrated in Fig. 4, the QRL model consistently outperforms both QNN and CNN across all user settings, showing a significant performance gain as the number of users grows. For instance, while all models start around 12 bps/Hz at  $T = 2$ , the QRL curve rises sharply, reaching nearly 20 bps/Hz at  $T = 10$ , whereas QNN and CNN achieve only about 17.2 bps/Hz and 15.8 bps/Hz, respectively. This result reveals that our proposed QRL framework exhibits better scalability, particularly in the targeted multi-user mMIMO environment, offering not only improved throughput but also robust scalability.

In addition, Fig. 5 presents the average sum rate difference across three methods for 6 users and  $\text{SNR} = 20$  configurations. The QRL model consistently achieves the highest performance across all antenna settings, starting approximately 8.2 bps/Hz at  $T = 6$  and climbing to nearly 14.7 bps/Hz at  $T = 16$ . This indicates that QRL leverages the spatial degrees of freedom provided by additional antennas more effectively than its classical and QNN-based counterparts. The QNN baseline performs better than CNN, scaling smoothly with more antennas, yet still falls short of QRL's throughput gains. There is also a noticeable performance gap between QRL and the benchmarks as the number of antennas increases, illustrating QRL's scalability in large-antenna regimes. Now we can safely state that the QRL model exhibits scalability in both antenna-wise and user-wise dimensions.

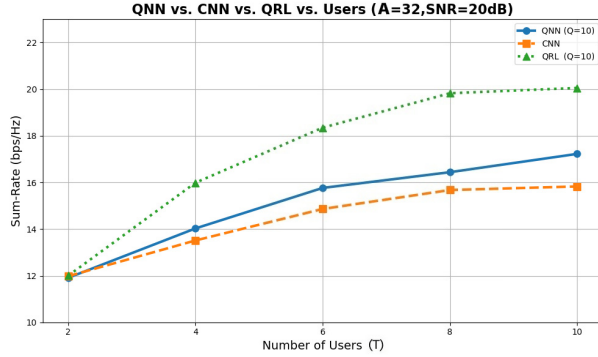


Fig. 4: Comparison of sum-rate performance versus number of users for QNN, CNN, and QRL under  $A=32$ ,  $\text{SNR}=20$  dB, showing the scalability of QRL in user number dimension.

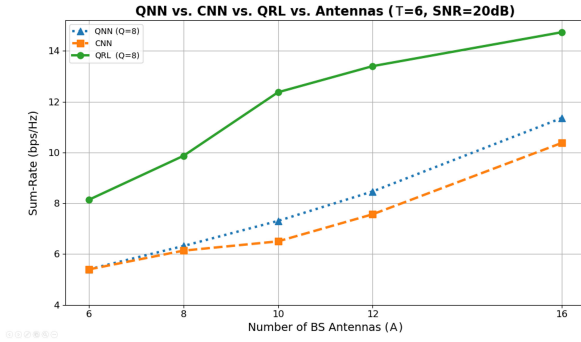


Fig. 5: Sum-rate versus number of BS antennas for QNN, CNN, and QRL under  $T = 6$ ,  $\text{SNR}=20$  dB, showing QRL's scalability in antenna number dimension.

Finally, we investigate the performance concerning different SNR configurations, while the other conditions remain the same. It can be seen that for two different user-antenna sets, the QRL consecutively outperforms its competitors, showing more rapid growth with increasing SNR in the initial state and saturating at higher sum-rate levels. Note that for the limited configuration, where 6 users and 8 antennas are included, the QRL model has achieved a higher average sum rate level after the SNR increased by more than 5 dB compared to the QNN and CNN under a better configuration. It demonstrates the QRL model reacts more sensitively in terms of exploiting high-SNR environments to maximize throughput.

## V. CONCLUSION

This paper presents a Grover's search-inspired QRL method for user scheduling in mMIMO systems. We designed a quantum gate-based circuit that adheres to the principles of reinforcement learning, efficiently exploring the scheduling space and amplifying high-reward policies through amplitude amplification. This design allows the system to overcome the scalability and complexity barriers of classical methods while achieving a higher average throughput. It has been validated by comparison with QNN and CNN benchmarks across diverse settings, including user and antenna scaling, and varying SNR configurations, demonstrating that the model can not only

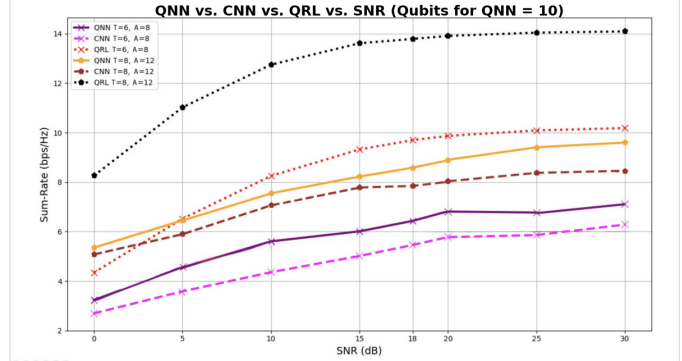


Fig. 6: Sum-rate versus SNR for QNN, CNN, and QRL under different user-antenna configurations, highlighting QRL's sensitivity and scalability in high-SNR environment.

improve average sum rate but also maintain robustness and adaptability in high-dimensional environments. These findings show the potential of Grover-inspired QRL as a promising approach for intelligent resource allocation in 5G/B5G networks and future quantum communication networks.

## REFERENCES

- [1] D. Sabat, P. Pattanayak, A. Kumar, and G. Prasad, "User scheduling with limited feedback for multi-cell mu-massive mimo fdd networks deployment: From performance tradeoff perspective," *International Journal of Communication Systems*, vol. 38, no. 5, p. e70021, 2025.
- [2] C. Luo, J. Ji, Q. Wang, X. Chen, and P. Li, "Channel state information prediction for 5g wireless communications: A deep learning approach," *IEEE transactions on network science and engineering*, vol. 7, no. 1, pp. 227–236, 2018.
- [3] X. Yu, J. Guo, X. Li, and S. Jin, "Deep learning based user scheduling for massive mimo downlink system," *Science China Information Sciences*, vol. 64, no. 8, p. 182304, 2021.
- [4] G. Bu and J. Jiang, "Reinforcement learning-based user scheduling and resource allocation for massive mu-mimo system," in *2019 IEEE/CIC International Conference on Communications in China (ICCC)*. IEEE, 2019, pp. 641–646.
- [5] X. Huang, R. Fan, M. Chakraborty, A. Nag, and A. Mukherjee, "Quantum deep learning for massive mimo user scheduling," *arXiv preprint arXiv:2508.03327*, 2025.
- [6] D. Bulger, W. P. Baritompa, and G. R. Wood, "Implementing pure adaptive search with grover's quantum algorithm," *Journal of optimization theory and applications*, vol. 116, no. 3, pp. 517–529, 2003.
- [7] X. Li, S. Jin, H. A. Suraweera, J. Hou, and X. Gao, "Statistical 3-d beamforming for large-scale mimo downlink systems over rician fading channels," *IEEE Transactions on Communications*, vol. 64, no. 4, pp. 1529–1543, 2016.
- [8] X. Li, X. Yu, T. Sun, J. Guo, and J. Zhang, "Joint scheduling and deep learning-based beamforming for fd-mimo systems over correlated rician fading," *IEEE Access*, vol. 7, pp. 118 297–118 309, 2019.
- [9] A. Maaref and S. Aissa, "Capacity of mimo rician fading channels with transmitter and receiver channel state information," *IEEE transactions on wireless communications*, vol. 7, no. 5, pp. 1687–1698, 2008.
- [10] C. Sun, X. Gao, S. Jin, M. Matthaiou, Z. Ding, and C. Xiao, "Beam division multiple access transmission for massive mimo communications," *IEEE Transactions on Communications*, vol. 63, no. 6, pp. 2170–2184, 2015.
- [11] P. R. Giri and V. E. Korepin, "A review on quantum search algorithms," *Quantum Information Processing*, vol. 16, no. 12, p. 315, 2017.
- [12] D. J. Shepherd, "On the role of hadamard gates in quantum circuits," *Quantum Information Processing*, vol. 5, no. 3, pp. 161–177, 2006.